Continuously Tunable Time Delay Using an Optically Pumped Linear Chirped Fiber Bragg Grating

Hiva Shahoei, *Student Member, IEEE*, Ming Li, *Member, IEEE*, and Jianping Yao, *Senior Member, IEEE, Fellow, OSA*

***Abstract*—A simple method to achieve a large and tunable time delay of an optical signal by using a linearly chirped fiber Bragg grating (LCFBG) written in an erbium–ytterbium (Er/Yb) codoped fiber is proposed and demonstrated. The group delay response of the LCFBG can be tuned by optically pumping the LCFBG with different pumping powers, which leads to the tuning of the time delay. An LCFBG written in an Er/Yb codoped fiber is fabricated. A continuously tunable time delay up to 200 ps for a Gaussian pulse with a full-width at half-maximum of 7.6 GHz is experimentally demonstrated. The influence of the dispersion, the magnitude and group delay ripples of the LCFBG on the time delay performance, and also the stability of operation are investigated.**

***Index Terms*—Linearly chirped fiber Bragg grating (LCFBG), microwave photonics, optical communications, time delay.**

I. Introduction

THE ability to control the time delay of an optical signal or pulse is an interesting topic which can find many applications such as in optical communications, optical signal processing, all-optical microwave filtering, and optically controlled phased array beamforming. For many applications, it is also required that the time delay be achieved for a signal or pulse with a large bandwidth.

Different schemes have been proposed for the implementation of continuously tunable time delay. The techniques for achieving tunable time delay have been widely studied under the concept of slow light, with different approaches such as electromagnetically induced transparency [1], coherent population oscillation [2]–[4], and stimulated Brillouin scattering (SBS) [5]–[7]. Among the numerous techniques, the one based on the SBS has attracted much attention since a low-power pump is needed to generate a large time delay. However, because of the narrow intrinsic bandwidth of the SBS, its applications are limited for narrowband signals or the system becomes complicated to satisfy the broadband operation requirement [8]–[10].

Fiber Bragg gratings (FBGs) are key fiber-optic components that can find many applications in optical communications systems such as optical filtering, group velocity dispersion compensation, and dispersion slope compensation. Recently, FBGs have been used to generate slow light to achieve optical time delays. In [11], the slow light properties of gap solitons in an apodized FBG are reported. By introducing a high-power signal, the optical nonlinearity would induce an index change in the FBG; thus, the time delay can be tuned by varying the optical power of the optical signal. Since this approach requires a very high optical power for the optical signal ($\sim$2 kW), its practical application is thus limited. In [12], a tunable time delay is achieved by thermally shifting the reflection edge of a uniform FBG written in an erbium–ytterbium (Er/Yb) codoped fiber. By introducing an optical pump, the reflection phase of the FBG tends to vary rapidly near the band edge and the time delay close to the band edge becomes appreciable [13]. By changing the pump power, the spectral bandwidth of the FBG is shifted, and as a result, the time delay from the FBG is varied. The amount of time delay achieved is 0.9 ns for an optical signal with a bandwidth of 200 MHz. The major limitation of this method is the limited bandwidth, which is not suitable for applications where a large bandwidth is needed.

A linearly chirped fiber Bragg grating (LCFBG) can provide a tunable time delay with a large bandwidth, and has been employed in optical communications systems, optical signal processing systems, and optically controlled phased array antennas [14]–[18]. In [14]–[17], the realization of a tunable time delay based on mechanical [14]–[16], or thermal [17] tuning of an LCFBG was demonstrated. For example, in [16], a right-angled triangle cantilever beam is used as the chirped fiber Bragg grating (CFBG) carrier to introduce a uniform strain gradient along the CFBG. A tunable dispersion from 178 to 2126 ps/nm corresponding to a 3-dB bandwidth from 0.42 to 5.04 nm is achieved mechanically. In the methods reported in [14]–[17], although the tunable range can be large, the tuning speed is very low. In addition, the stability of the system is also poor, especially for mechanical tuning. In [18], instead of employing mechanical or thermal tuning, the time delay is tuned by wavelength conversion based on four-wave mixing (FWM) in an optical fiber. Again, the system is complicated since a second light source with a high power is needed as a pump source to stimulate the FWM. A similar approach for achieving continuously tunable time delay is also proposed [19]. In the approach, the spectrum of an optical signal is broadened based on self-phase modulation, and the broadened spectrum is sliced by an optical filter. Due to the dispersion of an optical fiber, the time delay experienced by the sliced optical signal is different depending on the wavelength of the optical filter. The wavelength of the time-delayed signal is then reconverted back to the original wavelength by another spectral broadening operation

Manuscript received November 29, 2010; revised January 24, 2011; accepted March 14, 2011. Date of publication March 28, 2011; date of current version May 02, 2011. This work was supported by the Natural Science and Engineering Research Council of Canada.

The authors are with the Microwave Photonics Research Laboratory, School of Information Technology and Engineering, University of Ottawa, Ottawa, ON K1N 6N5, Canada (e-mail: jpyao@site.uottawa.ca).

Color versions of one or more of the figures in this paper are available online at http://ieeexplore.ieee.org.

Digital Object Identifier 10.1109/JLT.2011.2132754

and a second optical filter. The wavelength conversion can also be implemented using a parametric wavelength converter [20]. Clearly, the systems in [19] and [20] are complicated, and the tuning speed of the time delay is limited due to the slow tuning speed of the optical filter.

In this paper, a simple technique to achieve a continuously tunable time delay by using an LCFBG inscribed in an Er/Yb codoped fiber is proposed and experimentally demonstrated. By introducing a pump power to the LCFBG written in an Er/Yb codoped fiber, the temperature in the fiber would increase, which would lead to the change of the period and refractive index profiles of the LCFBG. Consequently, the group delay response would change, resulting in the change of the time delays. The key difference between this technique and the technique in [12] is that here an LCFBG is employed and the reflection is in the LCFBG band rather than in the band edge, which enables the system to provide a tunable time delay with a large bandwidth. In addition, the tuning speed is much faster than the approaches using thermal [14]–[16] or mechanical [17] tuning. Further more, the undesirable birefringence effects existing in the mechanical tuning technique can also be avoided using optical pumping. An LCFBG in an Er/Yb codoped fiber is fabricated. The use of the LCFBG to generate a tunable time delay by changing the pump power is investigated.

The paper is organized as follows. In Section II, the tuning mechanism of an LCFBG based on optical pumping is analyzed. The relationship between the pumping power and the time delay is established. In Section III, an experiment is performed. The use of the LCFBG to achieve a tunable time delay is experimentally demonstrated. A continuously tunable time delay as large as 200 ps is obtained for an input optical Gaussian pulse with a full-width at half-maximum (FWHM) of 7.6 GHz. In Section IV, the performance of the time delay system is evaluated, including the influence of the magnitude and group delay ripples on the time delay accuracy, the effect of the dispersion of the LCFBG on the time-delayed signals, and the stability of the operation. A summary of the important features of different schemes using an FBG or an LCFBG is provided. A conclusion is drawn in Section V.

II. Principle

It is well known that a chirp in the period of an LCFBG would lead to the broadening of the reflection spectrum. The broadened spectrum $\Delta\lambda_{\text{chirp}}$ is expressed as [21]

$$\Delta\lambda_{\text{chirp}} = 2n_{\text{eff}}\Delta\Lambda_{\text{chirp}}. \tag{1}$$

where n_{eff} is the effective refractive index of the grating and $\Delta\Lambda_{\text{chirp}}$ is the chirp in the period of the LCFBG. The group delay response of an LCFBG is a function of wavelength. A light wave reflected from the LCFBG would experience a time delay $\tau(\lambda)$ for $2n_{\text{eff}}\Lambda_{\text{short}} < \lambda < 2n_{\text{eff}}\Lambda_{\text{long}}$ which is a function of wavelength [21]

$$\tau(\lambda) \approx \frac{\lambda_0 - \lambda}{\Delta\lambda_{\text{chirp}}} \times \frac{2L}{v_g} \tag{2}$$

where λ_0 denotes the central wavelength of the reflection spectrum, v_g is the average group velocity of the light in the LCFBG, and L is the length of the LCFBG. The time delay slope in the reflection bandwidth is given by

$$\frac{d\tau(\lambda)}{d\lambda} = \frac{-2L}{\Delta\lambda_{\text{chirp}}v_g}. \tag{3}$$

The characteristics of a continuously pumped LCFBG can be explored by modeling the pumping effect in a doped fiber [22]. When a doped fiber is optically pumped, two effects are introduced: the first is the change of the refractive index and the second is the longitudinal expansion of the fiber. Since the second effect amounts to less than 2% of the first one, only the refractive index change due to the thermo-optic effect is considered in this paper.

First, it is assumed that the fiber is unjacketed and is long enough such that the z-dependence of the temperature profile is time invariant (z is the position along the fiber). The temperature distribution $T(r,t)$ should satisfy the heat conduction equation [23]

$$\rho c_v \frac{\partial T(r,t)}{\partial t} - k\nabla^2 T(r,t) = \eta P_v(r) \tag{4}$$

where ∇^2 is the Laplace operator, r is the radius position of the fiber, η is the fraction of the absorbed pump power which is turned to heat, k is the thermal conductivity of the fiber, ρ is the density of the fiber material, c_v is the specific heat, and P_v is the average pump power absorbed per unit volume. Since we need steady-state condition for practical case, it is useful to derive the steady-state temperature change relation. In this case, the time derivative in (4) is zero. For solving this equation, two boundary conditions should be considered. The first one is energy conversation. If the cooling is due to natural air convection, the heat flowing out of the fiber at $r = b$, where b is the outer radius of the unjacketed fiber, is proportional to the temperature difference between the fiber and the surrounding air. This proportionality factor is named as heat transfer coefficient h. The second boundary condition is that at $t = 0$, the temperature distribution is equal to the initial distribution $T(r, t = 0)$. In this regard, s is the absorption boundary, the radius of the step initial profile of $T(r, t = 0)$. Here, $\Delta T(r,t) = T(r,t) - T_0$ is the temperature rise in the profile, and T_0 denotes the equilibrium temperature of the surrounding medium. By considering these two boundary conditions, the steady-state temperature rise profile can be written as [22]

$$\Delta T_{ss}(r) = \frac{\eta P_v s^2}{2bh} - \frac{\eta P_v s^2}{2k}\ln\left(\frac{r}{b}\right). \tag{5}$$

To obtain the steady-state index change due to ΔT_{ss}, the absorbed power per unit volume can be expressed as

$$P_v(z) = \frac{-1}{\pi s^2} \times \frac{dP_p(z)}{dz} \tag{6}$$

where $P_p(z)$ is the pump power distribution along the fiber (which depends on the input pump power, the dopant absorption properties, and the pump mode size). The z dependence of ΔT_{ss} can be approximated by inserting (6) into (5) and retaining only the first term. So that the steady-state thermal index change is given by

$$\Delta n_{ss}(z) = \frac{\partial n}{\partial T} \times \frac{-\eta}{2\pi bh} \times \frac{dP_p(z)}{dz} \tag{7}$$

where $\partial n/\partial T$ is the index temperature coefficient. Therefore, depending on the pump power distribution, the refractive index of the fiber would change along the LCFBG. If the introduced pump is not strong enough to be distributed along all the length of the LCFBG, it will be distributed just in the periods that are located closer to the pumping power. When the LCFBG is optically pumped from the red end (i.e., with a longest period) and all the pump power is absorbed before the blue end (i.e., with a shortest period), the temperature at the red end of the LCFBG is increased to shift the second reflection edge to a longer wavelength while the first edge is fixed. By inserting (7) into (1) and (2), we can establish the relationship between the pumping power and the time delay given by

$$\tau(\lambda) = \frac{\left[n_s\Lambda_s + \left(n_l - \frac{\partial n}{\partial T} \times \frac{\eta}{2\pi bh} \times \frac{dP_z(z)}{dz}\Big|_{z=0}\right)\Lambda_l - \lambda\right]}{n_s\Lambda_s - \left(n_l - \frac{\partial n}{\partial T} \times \frac{\eta}{2\pi bh} \times \frac{dP_p(z)}{dz}\Big|_{z=0}\right)\Lambda_l} \times \frac{L}{v_g} \tag{8}$$

where Λ_s and Λ_l are the shortest and longest periods of the LCFBG, respectively, and n_s and n_l are the corresponding refractive indexes. Also, the slope of the time delay in the reflection band can be written as

$$\frac{d\tau(\lambda)}{d\lambda} = \frac{-L}{\left[n_s\Lambda_s - \left(n_l - \frac{\partial n}{\partial T} \times \frac{\eta}{2\pi bh} \times \frac{dP_p(z)}{dz}\Big|_{z=0}\right)\Lambda_l \times v_g\right]}. \tag{9}$$

Thus, it can be seen that when an LCFBG is pumped from its red end, the absolute value of the slope of the group delay response is decreased, as given by (9), and thus the achieved time delay of an optical signal over a specific band is increased.

III. Experimental Results

A ~8 cm long LCFBG is fabricated with UV scanning beam technique using a linearly chirped phase mask with a chirp rate of 0.056 nm/cm in the experiment. The fiber used to fabricate the LCFBG is a hydrogen-loaded Er/Yb codoped fiber. The central wavelength of the LCFBG is 1558.38 nm and the reflection FWHM is about 0.45 nm. Fig. 1 shows the experimental setup to achieve a tunable time delay by using an optically pumped LCFBG. The system consists of a tunable laser source (TLS), a Mach–Zehnder modulator (MZM), an LCFBG, a 980-nm laser diode (LD), an 3-port optical circulator, a photodetector (PD), a signal generator [Agilent N4901B Serial Bit Error Rate Tester (BERT)], and an oscilloscope (Agilent 86116A). A light wave from the TLS is sent to the MZM. The wavelength of the light wave is tuned at 1558.5 nm. A Gaussian pulse with an FWHM of 7.6 GHz generated by the signal generator is applied to the MZM via the RF port to modulate the light wave. The LCFBG is pumped by the 980-nm LD; by increasing the injection current of the pump laser, the introduced pump power is increased. The Gaussian pulse is reflected back from the LCFBG and applied to the PD via the optical circulator. In the experiment, the LCFBG is fixed on an optical table to minimize the instability caused by the environmental changes. The tunable time delay of the reflected signal is measured by the oscilloscope.

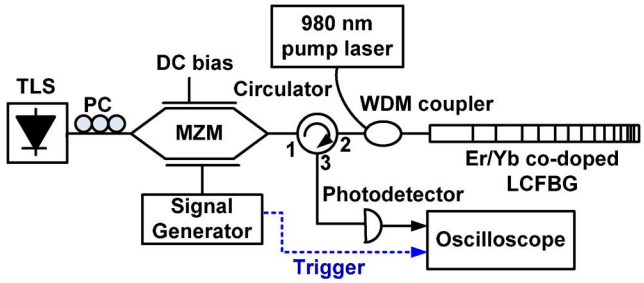

Fig. 1. Experimental setup to achieve a continuously tunable time delay. (TLS: tunable laser source, MZM: Mach–Zehnder modulator, PC: polarization controller, WDM: 980/1550 nm wavelength division multiplexer).

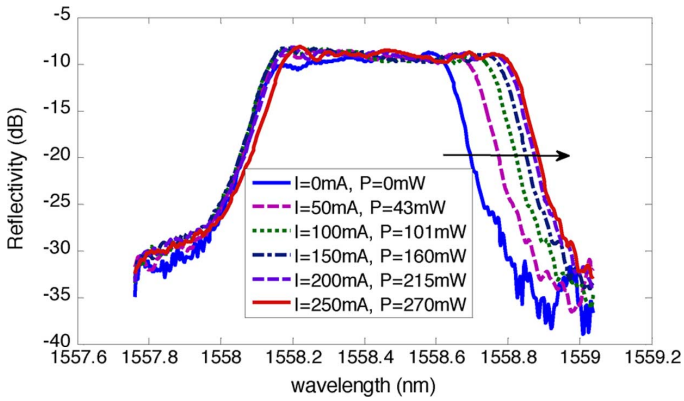

Fig. 2. Reflection spectra of the LCFBG pumped by a 980-nm LD with different pump powers.

As discussed in Section II, in a doped fiber, the core refractive index changes as a consequence of the variation of the pump power. The reflection edge wavelengths of an LCFBG are linearly proportional to the core refractive indexes of the shortest and longest periods, as given by (1). In our experiment, the power of the pump laser is small such that the LCFBG at the blue end is almost not pumped. Since the LCFBG is pumped from the red end, as explained in Section II, by increasing the pump power, the second edge of the LCFBG is shifted to a longer wavelength while the first edge is kept fixed. Fig. 2 shows the measured reflection spectra of the LCFBG with different pump powers. When the injection current of the pump laser is increased from 0 to 250 mA with a step of 50 mA (the corresponding pump power is from 0 to 270 mW), the second reflection edge is shifted to a longer wavelength with a wavelength shift of 0.2 nm. Fig. 3 shows the group delay responses of the LCFBG. As can be seen in Fig. 3, by increasing the pump power, the slope of the group delay is decreased, and therefore, the achieved time delay of an optical signal at a specific wavelength is increased.

Fig. 4 shows the detected signals reflected back from the LCFBG with different time delays for different pump powers. By increasing the injection current of the pump laser from 0 to 250 mA (the corresponding pump power from 0 to 270 mW), a time delay that is continuously tunable up to 200 ps is achieved. The measured intensity of the time-delayed signals shown in Fig. 4 is normalized to unity. The time-delayed signals experience some distortions because of the magnitude and group delay ripples of the LCFBG.

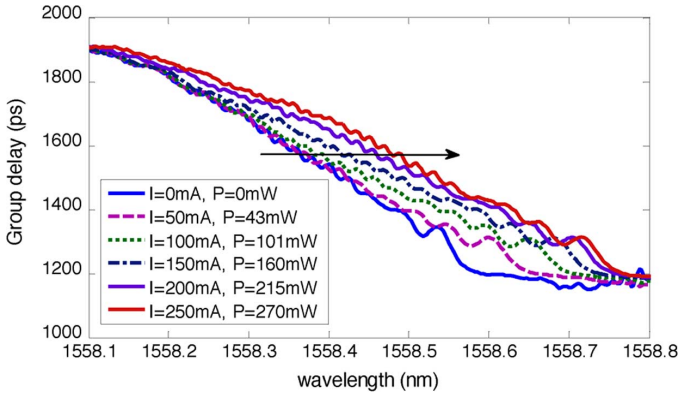

Fig. 3. Group delay responses of the LCFBG pumped by a 980-nm LD with different pump powers.

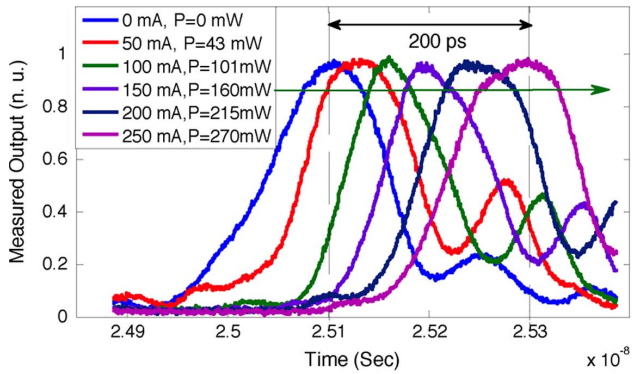

Fig. 4. Detected signals reflected from the pumped LCFBG with different pump powers.

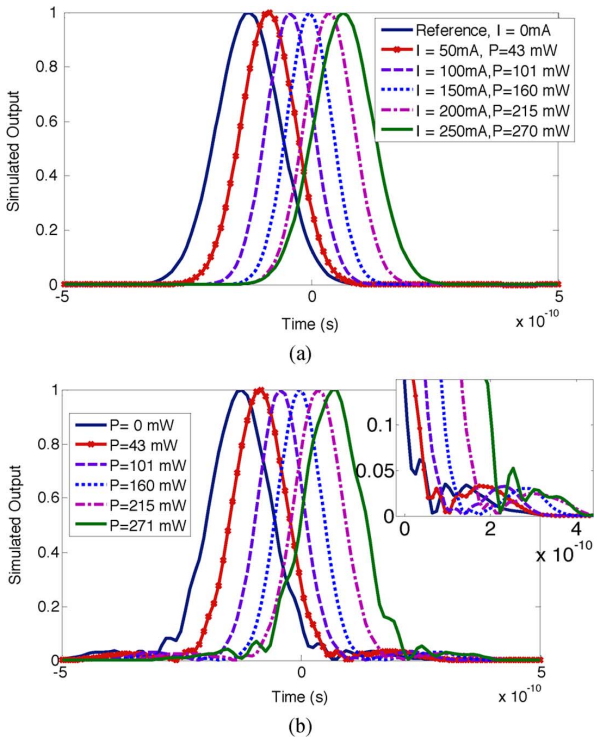

Fig. 5. Simulated time-delayed signals reflected from (a) an ideal LCFBG and (b) the experimented nonideal LCFBG pumped with different powers. The case with no pumping is considered as a reference. The inset in (b) shows a zoom-in view of the right edges of the simulated outputs.

IV. Discussions

A. Influence of the Magnitude and Group Delay Ripples on the Time Delay Performance

An ideal LCFBG would exhibit a constant magnitude and linear group delay characteristics over a large bandwidth. However, because of errors in grating periods and refractive index modulation raised in the grating fabrication process, ripples in the magnitude and group delay spectra would always exist. Usually, the impact of the ripples on the delayed signals can be evaluated by modeling the ripples as periodic functions that are superimposed on the magnitude and time delay responses of an ideal LCFBG [24]. By considering the frequency response of an LCFBG as $R = |R| \cdot e^{-j\theta}$, the reflectivity and its associated time delay can be written as a function of wavelength

$$|R(\lambda)| = (1 - r_1) + r_1 \cdot \sin\left(\frac{2\pi}{p} \cdot \lambda\right) \tag{10}$$

$$\tau(\lambda) = a_1 \cdot \lambda + a_2 + b_1 \cdot \sin\left(\frac{2\pi}{p} \cdot \lambda\right) \tag{11}$$

where r_1 and b_1 are the amplitudes of the reflectivity and the time delay ripples, respectively, p is the period of the ripples, and a_1 and a_2 are two constants. Since

$$\theta(\lambda) = -2\pi c \int \left(\frac{\tau(\lambda)}{\lambda^2}\right) d\lambda \tag{12}$$

where c is the speed of light in vacuum, by integrating (11), we can find the phase response. Thus, by having the magnitude and phase responses of a nonideal LCFBG with ripples in the reflectivity and group delay responses, we can investigate the influence of the ripples on the time-delayed signals. Fig. 5 shows the simulated time-delayed signals by an ideal LCFBG with different pump powers. As can be seen from Fig. 5(a), by increasing the pump power, the time delay is increasing. The shape of the Gaussian pulses does not change after reflected from the ideal LCFBG. Fig. 5(b) shows the simulated time-delayed signals based on the measured reflection and time delay spectra of the fabricated LCFBG for different pump powers. The periods and amplitudes of the ripples as well as the constants (i.e., a_1 and a_2) in (11) and (12) are obtained based on the measured reflection and time delay spectra, shown in Figs. 2 and 3. As can be seen from Fig. 5(b), because of the ripples in the reflection and group delay spectra, the time-delayed signals experience some distortions. The amount of distortion depends on the amplitude and the period of the ripples.

To investigate the influence of the reflectivity ripples on the time-delayed signals, a linear group delay is considered. In Fig. 6(a), the amplitude of the ripples r_1 is constant (1.2 dB). The period of the ripples of the reflectivity spectrum is increased from 7.5 to 60 pm. As can be seen in Fig. 6(a), the output does not have a symmetric spectrum. By increasing the period of the ripples, the first left sidelobe gets closer to the main lobe and its amplitude becomes smaller. In addition to the change of the amplitude and position of the sidelobe, the stimulated signal experiences more distortions. For example,

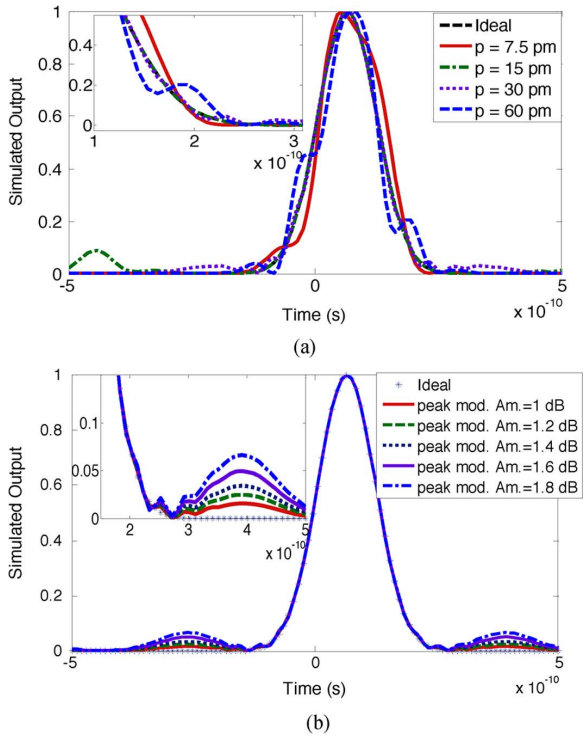

Fig. 6. Simulated time-delayed signals reflected from a nonideal LCFBG with linear time delay but modulated reflection spectra with (a) different ripple periods and (b) different peak to peak ripple amplitudes. The insets show the zoom-in views of the right edges of the simulated outputs.

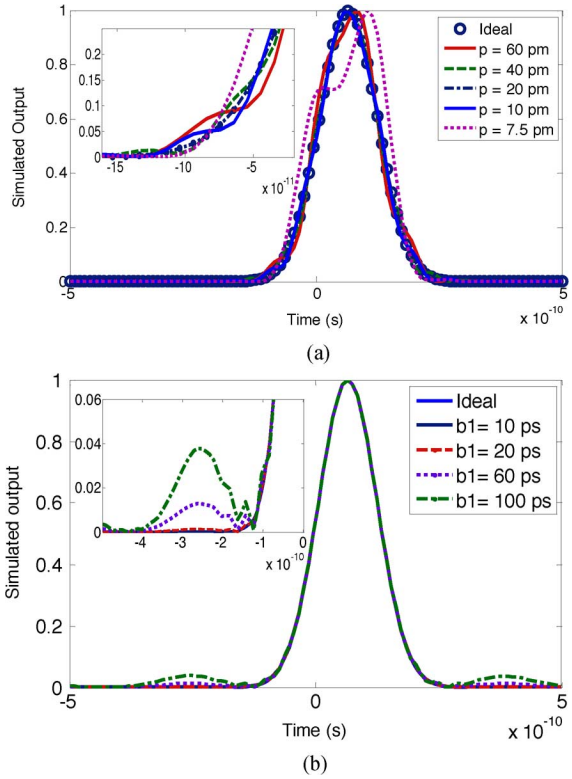

Fig. 7. Simulated time-delayed signals for a nonideal LCFBG with a constant reflectivity but modulated time delay response with (a) different ripple periods and (b) different ripple amplitudes. The insets show the zoom-in views of the left edges of the simulated outputs.

the output gets broader for $p = 7.5$ pm. In Fig. 6(b), the period of the ripples is constant (25 pm) and the peak amplitude of the ripples is increased from 1 to 1.8 dB. By increasing the amplitude of the ripples, the locations of the sidelobes are fixed but the amplitudes become larger. It can be seen that the distortion is predictable when just the amplitude of the ripples in the reflectivity changes, but it is more complicated when its period changes. It is because the maximum and minimum of the ripples fall in different wavelengths by changing the period.

To study the effect of group delay ripples on the time-delayed signals, a constant reflectivity is considered. In Fig. 7(a), the amplitude of the group delay ripples is constant ($b_1 = 20$ ps) and the period is decreased from 60 to 7.5 pm. As can be seen, we have some distortions in the edge of the signal. The distortion is worst when the period is smallest since time delay changes a lot within a small wavelength band. For $p = 7.5$ pm, the peak wavelength is shifted and the pulse is distorted significantly near the peak area, also the output pulse gets broader about 31%. Fig. 7(b) shows the simulated time-delayed signals for a constant ripple period (25 pm) but different ripple amplitudes in the group delay response. By increasing the ripple amplitude, the locations of the sidelobes are fixed but the amplitudes become larger. It can be seen that the effect of the amplitude ripples in the group delay is not very serious, since for the $b_1 = 60$ ps, which is a large amount, the sidelobe amplitude is below 0.02. Therefore, depending on the amplitude and period of the ripples in the reflection and time delay spectra, the time-delayed signal would be distorted and the effects of the periods of the ripples are much higher than theirs amplitude.

B. Effect of the Dispersion of the LCFBG on the Time-Delayed Signals

We assume the input optical pulse as $g(t) = \exp(-t^2/\tau_0^2)$, where τ_0 is the half bandwidth at $1/e$ maximum. Its Fourier transform is given by $G(\omega) = \sqrt{\pi}\tau_0 \exp(-\tau_0^2\omega^2/4)$, where ω denotes the optical angular frequency. The LCFBG can be modeled as a linear time-invariant system with a transfer function given by

$$H(\omega) = \exp\left[-j\left(\frac{\ddot{\Phi}\omega^2}{2}\right)\right] \tag{13}$$

where $\ddot{\Phi}$ donates the second-order dispersion (ps^2) of the LCFBG and $j = \sqrt{-1}$. Here, the higher orders of dispersion are neglected. By increasing the pump power, the slope of the group delay decreases, and thus the $\ddot{\Phi}$ decreases. Here, by increasing the pump power from 0 to 270 mW, the $\ddot{\Phi}$ decreases from 2003.7 to 1438.8 ps^2. By having the transfer function of the LCFBG for different pump powers (different dispersion values) and applying the Gaussian pulse to the LCFBG, the output pulse can be simulated. Fig. 8 shows the simulated outputs of the system for different pump powers. Here, the LCFBG is considered ideal without ripples. It can be seen that the simulated output pulses experience the broadening as the result of the dispersion of the LCFBG. As the dispersion is higher, the broadening is more.

There is a tradeoff between the tunable range of the time delay and the broadening of the input pulse. By increasing the disper-

TABLE I
COMPARISONS BETWEEN THE PREVIOUS SCHEMES OF TUNABLE TIME DELAYS USING FBG IN THEIR STRUCTURES

Different schemes for the generation of a tunable time delay	Using a LCFBG			Using a pumped FBG	Using a pumped LCFBG
	Changing the period of the LCFBG [15]	Changing the refractive index of the LCFBG [17]	Wavelength-conversion and dispersion-induced time delay [18]	Changing the refractive index of the FBG [12]	Changing the refractive index of the LCFBG (our proposed technique)
Method of Tuning	Mechanical tuning	Thermal tuning	Idler wavelength tuning	Pump power tuning	Pump power tuning
Tunable time delay	120 ps	86 ps	200 ps	850 ps	200 ps
Bandwidth	10 GHz	2 GHz	10 GHz	200 MHz	56 GHz
Tunable time-bandwidth product	1.2	0.172	2	0.17	11.2
Stability	Low as the achieved time delay depends on the bending of the LCFBG and the applied load, or the introduced heat		High as by changing the idler wavelength the time delay is achieved	Low as the carrier frequency should be tuned within a narrow bandwidth of the reflection edge of the FBG	High as the carrier frequency is tuned within a large bandwidth of the reflection band of the LCFBG
Tuning speed	Low as the change of the mechanical load or temperature or bending the FBG is not fast		Fast as the wavelength of a second laser can be tuned at a high speed	Fast as the pump power can be tuned at a high speed	
Fabrication complexity	Fairly low		High	Low	

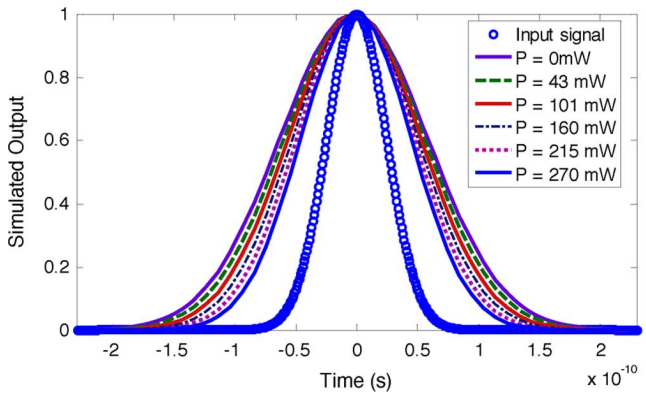

Fig. 8. Simulated time-delayed signals reflected from a nonideal LCFBG pumped with different pump powers, corresponding to different dispersion.

sion of the LCFBG, a greater tunable time delay is achieved but the output pulse would experience larger broadening.

C. Stability

The stability of the proposed system is also investigated. To do so, the reflection and group delay spectra of the LCFBG are measured every 5 min when the injection current of the LD is $I = 250$ mA or equivalently an pumping power of $P = 270$ mW). The results are shown in Fig. 9. As can be seen, after 25 min, the reflectivity and the group delay responses of the LCFBG do not have any visible changes, a high stable operation is confirmed.

D. Bandwidth of the System

The bandwidth of our system is limited by the reflection bandwidth of the LCFBG. In our experiment, since the reflection bandwidth of the LCFBG is 0.45 nm or equivalently 56 GHz, the bandwidth of the entire system is thus 56 GHz. By using a phase mask with a wider bandwidth, the bandwidth of the LCFBG can be increased, and the entire bandwidth of the system is also increased.

A comparison of the important features of different schemes using an FBG or an LCFBG in their structures to achieve a tunable time delay is summarized in Table I. A figure of merit to evaluate the performance of a time delay system is the time-bandwidth product. As can be seen, among the different techniques, our proposed solution provides the largest tunable time-bandwidth product which is 11.2. The proposed system also provides good performance including high operation stability, large tunability, and low fabrication complexity.

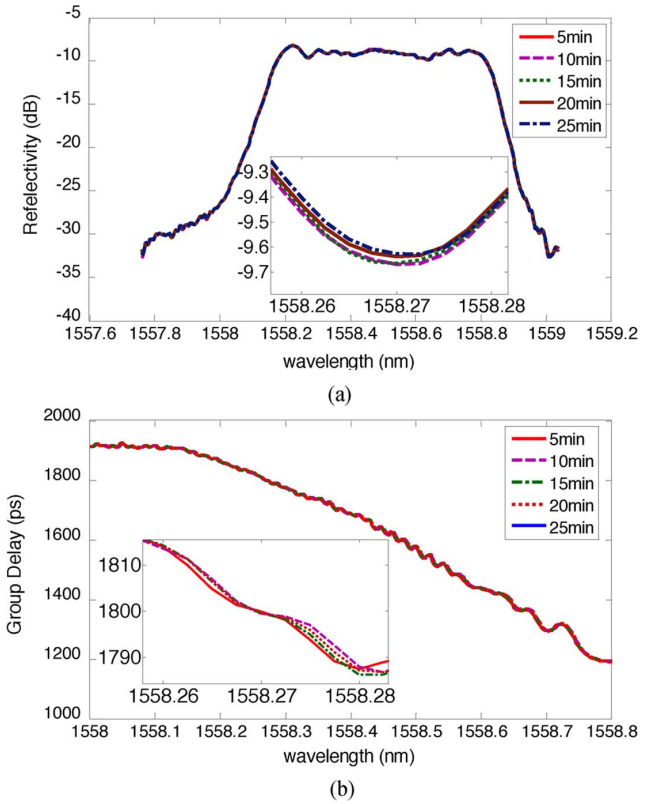

Fig. 9. Experimental measurement of the group delay response to evaluate the stability of the system. (a) Reflectivity and (b) group delay responses of the LCFBG pumped with $I = 250$ mA at different times. The inset shows a zoom-in views of the reflectivity and group delay responses.

V. Conclusion

A simple technique to achieve a continuously tunable time delay with a large tunable range was proposed and experimentally demonstrated. The key component in the proposed system is the LCFBG, which was fabricated in an Er/Yb codoped fiber. By optically pumping the LCFBG, the group delay response of the LCFBG was changed, leading to the change of the time delay. A theoretical analysis was performed, in which the relationship between the pumping power and the time delay was established. An experiment was then performed. A continuously tunable time delay as large as 200 ps was achieved. A figure of merit to evaluate the performance of a time delay system is the time-bandwidth product. For the proposed system, a tunable time-bandwidth product as large as 11.2 was achieved. The bandwidth of the proposed system was 56 GHz, which was limited by the reflection bandwidth of the LCFBG. By using a wider bandwidth LCFBG, the entire bandwidth of the system could be increased. The effect of the dispersion of the LCFBG on the time-delayed signals was evaluated. By increasing the dispersion of the LCFBG, a greater time delay could be achieved but the output pulse would experience larger broadening. The effect of the reflectivity and group delay ripples of the LCFBG on the time delay performance of the system was also investigated. It was shown that the reflectivity and group delay ripples would lead to the distortions to the time-delayed signals, and the amount of distortions in the time-delayed signals depends on the values of the period and amplitude of the ripples.

Acknowledgment

The authors would like to thank the loan of the linearly chirped phase mask by Prof. J. Albert at the Department of Electronics of Carleton University.

References

[1] L. V. Hau, S. E. Harris, Z. Dutton, and C. H. Behroozi, "Light speed reduction to 17 metres per second in an ultracold atomic gas," *Nature*, vol. 397, no. 6720, pp. 594–598, Feb. 1999.

[2] M. S. Bigelow, N. N. Lepeshkin, and R. W. Boyd, "Superluminal and slow light propagation in a room-temperature solid," *Science*, vol. 301, no. 5630, pp. 200–202, Jul. 2003.

[3] P. C. Ku, F. Sedgwick, C. J. Chang-Hasnain, P. Palinginis, T. Li, H. Wang, S. W. Chang, and S.-L. Chuang, "Slow light in semiconductor quantum wells," *Opt. Lett.*, vol. 29, no. 19, pp. 2291–2293, Oct. 2004.

[4] A. Schweinsberg, N. N. Lepeshkin, M. S. Bigelow, R. W. Boyd, and S. Jarabo, "Observation of superluminal and slow light propagation in erbium-doped optical fiber," *Europhys. Lett.*, vol. 73, no. 2, pp. 218–224, Jan. 2006.

[5] K. Y. Song, M. G. Herráez, and L. Thévenaz, "Observation of pulse delaying and advancement in optical fibers using stimulated Brillouin scattering," *Opt. Exp.*, vol. 13, no. 1, pp. 82–88, Jan. 2005.

[6] Y. Okawachi, M. S. Bigelow, J. E. Sharping, Z. Zhu, A. Schweinsberg, D. J. Gauthier, R. W. Boyd, and A. L. Gaeta, "Tunable all-optical delays via Brillouin slow light in an optical fiber," *Phys. Rev. Lett.*, vol. 94, no. 15, pp. 153902-1–153902-4, Apr. 2005.

[7] L. Xing, L. Zhan, S. Luo, and Y. Xia, "High-power low-noise fiber Brillouin amplifier for tunable slow-light delay buffer," *IEEE J. Quantum Electron.*, vol. 44, no. 12, pp. 1133–1138, Dec. 2008.

[8] Z. Zhu, A. M. C. Dawes, D. J. Gauthier, L. Zhang, and A. E. Willner, "12-GHz-bandwidth SBS slow light in optical fibers," presented at the Opt. Fiber Commun. Conf., Anaheim, CA, Mar. 2006, PDP1.

[9] K. Y. Song and K. Hotate, "25 GHz bandwidth Brillouin slow light in optical fibers," *Opt. Lett.*, vol. 32, no. 3, pp. 217–219, Feb. 2007.

[10] L. Yi, L. Zhan, W. Hu, and Y. Xia, "Delay of broadband signals using slow light in stimulated Brillouin scattering with phase-modulated pump," *IEEE Photon. Technol. Lett.*, vol. 19, no. 8, pp. 619–621, Mar. 2007.

[11] J. T. Mok, C. M. De Sterke, I. C. M. Littler, and B. J. Eggleton, "Dispersionless slow light using gap solitons," *Nat. Phys.*, vol. 2, no. 11, pp. 775–780, Oct. 2006.

[12] K. Qian, L. Zhan, H. Li, X. Hu, J. Peng, L. Zhang, and Y. Xia, "Tunable delay slow-light in an active fiber Bragg grating," *Opt. Exp.*, vol. 17, no. 24, pp. 22217–22222, Nov. 2009.

[13] T. Erdogan, "Fiber grating spectra," *J. Lightw. Technol.*, vol. 15, no. 8, pp. 1277–1294, Aug. 1997.

[14] D. B. Hunter, M. E. Parker, and J. L. Dexter, "Demonstration of a continuously variable true-time delay beamformer using a multichannel chirped fiber grating," *IEEE Trans. Microw. Theory Tech.*, vol. 54, no. 2, pp. 861–867, Feb. 2006.

[15] Y. Liu, J. Yang, and J. P. Yao, "Continuous true-time-delay beamforming for phased array antenna using a tunable chirped fiber grating delay line," *IEEE Photon. Technol. Lett.*, vol. 14, no. 8, pp. 1172–1174, Aug. 2002.

[16] X. Dong, P. Shum, N. Q. Ngo, C. C. Chan, C. Zhao, and J. H. Ng, "A largely tunable CFBG-based dispersion compensator with fixed center wavelength," *Opt. Exp.*, vol. 11, no. 22, pp. 2970–2974, Nov. 2003.

[17] M. Pisco, S. Campopiano, A. Cutolo, and A. Cusano, "Continuously variable optical delay line based on a chirped fiber Bragg grating," *IEEE Photon. Technol. Lett.*, vol. 18, no. 24, pp. 2551–2553, Dec. 2006.

[18] J. Liu, T. Cheng, Y. Yeo, Y. Wang, L. Xue, N. Zhu, Z. Xu, and D. Wang, "Hi-Fi all-optical continuously tunable delay with a high linear-chirp-rate fiber Bragg grating based on four-wave mixing in a highly-nonlinear photonic crystal fiber," *Opt. Comm.*, vol. 282, no. 22, pp. 4366–4369, Nov. 2009.

[19] Y. Okawachi, R. Salem, and A. L. Gaeta, "Continuous tunable delays at 10-Gb/s data rates using self-phase modulation and dispersion," *J. Lightw. Technol.*, vol. 25, no. 2, pp. 3710–3715, Dec. 2007.

[20] J. E. Sharping, Y. Okawachi, J. Howe, C. Xu, Y. Wang, A. E. Willner, and A. L. Gaeta, "All-optical, wavelength and bandwidth preserving, pluse delay based on parametric wavelength conversion and dispersion," *Opt. Exp.*, vol. 13, no. 20, pp. 7872–7877, Oct. 2005.

[21] R. Kashyap, *Fiber Bragg Gratings*, 2nd ed. New York: Academic, 1999, pp. 312–320.

[22] M. K. Davis, M. J. Digonnet, and R. Pantell, "Thermal effects in doped fibers," *J. Lightw. Technol.*, vol. 16, no. 6, pp. 1013–1023, Jun. 2003.

[23] C. Kittel and H. Kroemer, *Thermal Physics*, 2nd ed. New York: Freeman, 1980, pp. 424–430.

[24] K. Ensser, M. Durkin, M. N. Zervas, and R. I. Laming, "Influence of non-ideal chirped fiber grating characteristics on dispersion cancellation," *IEEE Photon. Technol. Lett.*, vol. 10, no. 10, pp. 1476–1478, Oct. 1998.

[25] J. Han, B. Seo, Y. Han, B. Jalali, and H. R. Fetterman, "Reduction of chromatic dispersion effects in fiber-wireless and photonic time-stretching system using polymer modulator," *J. Lightw. Technol.*, vol. 21, no. 21, pp. 1504–1510, Jun. 2003.

Hiva Shahoei (S'09) received the B.Sc. degree in electrical engineering from Tabriz University, Tabriz, Iran, in 2005, and the M.Sc. degree in electrical engineering from Tehran Polytechnic University, Tehran, Iran, in 2008. She is currently working toward the Ph.D. degree in electrical and computer engineering at the Microwave Photonics Research Laboratory, School of Information Technology and Engineering, University of Ottawa, Ottawa, ON, Canada.

Her current research interests include photonic processing of microwave signals, and slow and fast light and the applications in microwave photonics.

Ming Li (S'08–M'09) received the Ph.D. degree in electrical and electronics engineering from the University of Shizuoka, Hamamatsu, Japan, in March 2009.

In April 2009, he joined the Microwave Photonics Research Laboratory, School of Information Technology and Engineering, University of Ottawa, Ottawa, ON, Canada, as a Postdoctoral Research Fellow. His current research interests include advanced fiber Bragg grating and its applications to microwave photonics, ultrafast optical signal processing, arbitrary waveform generation, and optical microelectromechanical systems sensing.

Jianping Yao (M'99–SM'01) received the Ph.D. degree in electrical engineering from the Université de Toulon, Toulon, France, in 1997.

He joined the School of Information Technology and Engineering, University of Ottawa, ON, Canada, in 2001, where he is currently a Professor, the Director of the Microwave Photonics Research Laboratory, and the Director of the Ottawa-Carleton Institute for Electrical and Computer Engineering. From 1999 to 2001, he held a faculty position with the School of Electrical and Electronic Engineering, Nanyang Technological University, Singapore. He holds a Yongqian Endowed Visiting Chair Professorship with Zhejiang University, China. He spent three months as an Invited Professor in the Institut National Polytechnique de Grenoble, France, in 2005. His research has focused on microwave photonics, which includes all-optical microwave signal processing, photonic generation of microwave, mm-wave and terahertz, radio over fiber, ultrawideband over fiber, fiber Bragg gratings for microwave photonics applications, and optically controlled phased array antenna. His research interests also include fiber lasers, fiber-optic sensors, and biophotonics. He is the author or coauthor of more than 300 papers, including more than 170 papers in refereed journals and more than 130 papers in conference proceeding.

Dr. Yao is a registered Professional Engineer of Ontario. He is a Fellow of the Optical Society of America, and a Senior Member of the IEEE Photonics Society and the IEEE Microwave Theory and Techniques Society. He is an Associate Editor of the *International Journal of Microwave and Optical Technology*. He is on the Editorial Board of IEEE TRANSACTIONS ON MICROWAVE THEORY AND TECHNIQUES. He received the 2005 International Creative Research Award of the University of Ottawa. He was the recipient of the 2007 George S. Glinski Award for Excellence in Research. He was named University Research Chair in Microwave Photonics in 2007. He was a recipient of an NSERC Discovery Accelerator Supplements Award in 2008.